Available online at www.sciencedirect.com
SCIENCE DIRECT®
Journal of Sound and Vibration 267 (2003) 227–244
JOURNAL OF SOUND AND VIBRATION
www.elsevier.com/locate/jsvi

Symplectic analysis for periodical electro-magnetic waveguides

W.X. Zhong[a,1], F.W. Williams[b,*], A.Y.T. Leung[b]

[a] *Research Institute of Engineering Mechanics, Dalian University of Technology, Dalian 116024, China*
[b] *Department of Building and Construction, City University of Hong Kong, Tat Chee Avenue, Kowloon, Hong Kong, China*

Received 21 May 2002; accepted 18 October 2002

Abstract

Symplectic analysis is introduced into electro-magnetic waveguide theory, by using Hamiltonian system theory in which the transverse electric and magnetic field vectors are the dual vectors. The method can accommodate arbitrary anisotropic material and includes the interface conditions between adjacent segments of the waveguide. An *electro-magnetic stiffness matrix* is introduced which relates to the two ends of each segment of the waveguide. Both the pass- and stop-band stiffness matrices for plane waveguides with constant cross-section are given analytically and also a transformation matrix is given to permit abrupt changes of cross-section to occur. The variational principle is applied to obtain the segment combination algorithm needed to generate the electro-magnetic stiffness matrix related to the two ends of the fundamental periodical segment. Then the Wittrick–Williams algorithm is used to extract the eigenvalues. Thereafter, an energy band analysis is performed for a periodical waveguide, e.g., a grating, by using the symplectic eigensolutions.

1. Introduction

In civil and aeronautical engineering, analysis of wave propagation along a periodical structure shows that the eigenvalues exhibit *energy band* behaviour [1], such that a wave with frequency ω which is in a pass-band can propagate along the periodical structure, whereas otherwise ω is in a stop-band and the wave decays to zero over long distances. The energy analysis used to find pass- and stop-bands is also important in other practical disciplines. For example, electro-magnetic (opto-electronic) waveguide analysis has attracted extensive attention in recent years, e.g., see, Refs. [2–6], especially when used in optical integrated circuit analysis. Here periodical electro-

*Corresponding author. Tel.: +852-21942045; fax: +852-27887612.
E-mail address: bcfred@cityu.edu.hk (F.W. Williams).
[1] Visiting Professor at City University of Hong Kong.

0022-460X/03/$ - see front matter © 2002 Elsevier Science Ltd. All rights reserved.
doi:10.1016/S0022-460X(02)01451-7

magnetic waveguides, e.g., gratings, behave analogously to periodic structures and their band structure is the topic of the present paper, in which symplectic mathematical analysis is introduced for electro-magnetic waveguide analysis and shown to be effective. Hence, the numerical methods developed in computational structural mechanics can be applied, such as wave propagation along a periodical sub-structural chain. This interdisciplinary field offers many opportunities for further developments.

The Maxwell equation set is the foundation for this paper. For optical materials there is usually neither source nor current (i.e., $\rho = 0,\ \mathbf{j} = \mathbf{0}$) and the equations are given as [7–9]

$$\nabla \cdot \mathbf{D} = \mathbf{0}, \tag{1}$$

$$\nabla \cdot \mathbf{B} = \mathbf{0}, \tag{2}$$

$$\nabla \times \mathbf{E} = -\partial \mathbf{B}/\partial t = -\boldsymbol{\mu}\partial \mathbf{H}/\partial t, \tag{3}$$

$$\nabla \times \mathbf{H} = \partial \mathbf{D}/\partial t = \boldsymbol{\varepsilon}\partial \mathbf{E}/\partial t, \tag{4}$$

where $\mathbf{E}$ and $\mathbf{H}$ are, respectively, the electric and magnetic field vectors; $\mathbf{D}$ and $\mathbf{B}$ are electric displacement density and magnetic flux density vectors and; $\boldsymbol{\mu}$ and $\boldsymbol{\varepsilon}$ are permeability and permittivity matrices. The constitutive relations are

$$\mathbf{D} = \boldsymbol{\varepsilon}\mathbf{E}, \tag{5}$$

$$\mathbf{B} = \boldsymbol{\mu}\mathbf{H}, \tag{6}$$

where $\boldsymbol{\mu}$ for optical material can be regarded as in a vacuum, giving $\boldsymbol{\mu} = \mu_0\mathbf{I}_3$ with $\mu_0 = 4\pi \times 10^{-7}$ Herry, and $\boldsymbol{\varepsilon}$ is a (3×3) symmetric matrix. For isotropic material

$$\boldsymbol{\varepsilon} = \varepsilon\mathbf{I}_3, \quad \boldsymbol{\mu} = \mu_0\mathbf{I}_3. \tag{7a, b}$$

The Maxwell equations are formulated in the time domain, whereas the corresponding forms in the frequency domain are

$$\mathbf{H} = \mathbf{h}\mathrm{e}^{-\mathrm{i}\omega t}, \quad \mathbf{E} = \mathrm{i}\mathbf{e}\mathrm{e}^{-\mathrm{i}\omega t}, \tag{8}$$

where $\mathbf{e}(x, y, z, \omega)$ and $\mathbf{h}(x, y, z, \omega)$ are to be determined. Eqs. (3) and (4) transform to

$$\omega\mu_0\mathbf{h} = \mathbf{R} \cdot \mathbf{e}, \quad \omega\boldsymbol{\varepsilon} \cdot \mathbf{e} = \mathbf{R} \cdot \mathbf{h}, \tag{9a, b}$$

where

$$\mathbf{R} = \begin{bmatrix} 0 & -\partial/\partial z & \partial/\partial y \\ \partial/\partial z & 0 & -\partial/\partial x \\ -\partial/\partial y & \partial/\partial x & 0 \end{bmatrix} \tag{10}$$

is an operator matrix.

If S is the boundary surface of a finite domain V, the boundary condition for a perfect conductor is

$$\mathbf{n} \times \mathbf{e} = \mathbf{0}, \quad \mathbf{n} = \mathbf{i}_x l + \mathbf{i}_y m + \mathbf{i}_z n, \text{ on the boundary } S, \tag{11}$$

where $\mathbf{i}_x,\ \mathbf{i}_y$ and $\mathbf{i}_z$ are unit vectors along the right-hand Cartesian co-ordinate axes $x,\ y$ and z, while $l,\ m$ and n are the corresponding direction cosines. For an infinite domain the stop-band

condition is that the vectors decay fast enough in the far field, i.e.,

$$\mathbf{e}(\mathbf{r},\omega)\to o(|r|^{-1}),\qquad \mathbf{h}(\mathbf{r},\omega)\to o(|r|^{-1})\quad \text{when } |r|\to\infty, \tag{12}$$

where the vector fields **e** and **h** should be found from Eqs. (9a,b) and the respective boundary conditions.

For a finite domain V with perfect conductor boundary conditions, the variational principle can be expressed as

$$\Pi(\mathbf{e},\mathbf{h})=\mathrm{Re}\left\{\begin{array}{l}\int\int\int_V [\mathbf{h}^{\mathrm{H}}\cdot(\mathbf{R}\cdot\mathbf{e})-\mu_0\omega\mathbf{h}^{\mathrm{H}}\mathbf{h}/2-\omega\mathbf{e}^{\mathrm{H}}\boldsymbol{\varepsilon}\mathbf{e}/2]\,\mathrm{d}x\,\mathrm{d}y\,\mathrm{d}z\\ \quad+\int\int_S \mathbf{e}^{\mathrm{H}}\cdot(\mathbf{n}\times\mathbf{h})\,\mathrm{d}S\end{array}\right\},\quad \delta\Pi=0, \tag{13}$$

where superscript H denotes Hermitian transposition. The components of vectors **h** and **e** are treated as independently varying functions in the functional. Note that the boundary condition (11) is also the natural boundary condition derived from the variational principle [10].

When treating the problem of a suddenly changing cross-section, the natural boundary condition is a useful one. However, the alternative of a given tangential electric field vector boundary condition $\mathbf{e}_{sg}$ should also be considered. Thus the boundary condition (11) is revised to

$$\mathbf{n}\times(\mathbf{e}-\mathbf{e}_{sg})=0,\qquad \mathbf{n}=\mathbf{i}_x l+\mathbf{i}_y m+\mathbf{i}_z n\quad \text{along the boundary } S \tag{11'}$$

and the variational principle (13) must be revised to become

$$\Pi(\mathbf{e},\mathbf{h})=\mathrm{Re}\left\{\begin{array}{l}\int\int\int_V [\mathbf{h}^{\mathrm{H}}\cdot(\mathbf{R}\cdot\mathbf{e})-\mu_0\omega\mathbf{h}^{\mathrm{H}}\mathbf{h}/2-\omega\mathbf{e}^{\mathrm{H}}\boldsymbol{\varepsilon}\mathbf{e}/2]\,\mathrm{d}x\,\mathrm{d}y\,\mathrm{d}z\\ \quad+\int\int_S (\mathbf{e}-\mathbf{e}_{sg})^{\mathrm{H}}\cdot(\mathbf{n}\times\mathbf{h})\,\mathrm{d}S\end{array}\right\},\quad \delta\Pi=0, \tag{13'}$$

where $\mathbf{e}_{sg}$ is a given vector, i.e., it is not subject to variation. The verification of the variational principle is almost the same as for the natural boundary condition case. Thus, after the Maxwell equations have been satisfied in the domain, it only remains to perform the boundary surface integration

$$\int\int_S \delta\mathbf{h}^{\mathrm{H}}\cdot[\mathbf{n}\times(\mathbf{e}-\mathbf{e}_{sg})]\,\mathrm{d}S=0 \tag{13''}$$

and because of the arbitrariness of $\delta\mathbf{h}$, Eq. (11′) is reproduced, so that the verification is complete.

The variational principle (13) can be used for an arbitrary 3D domain and therefore can certainly be used for cylindrical domains, for which the longitudinal co-ordinate is z and the transverse co-ordinates are x and y. The lateral boundary conditions for a perfect conductor are $e_z=e_s=0$ and the normal component e_n is arbitrary, where $(\mathbf{n},\mathbf{s},\mathbf{z})$ is a right-hand Cartesian co-ordinate system, for which the outward normal can be expressed as

$$\mathbf{n}=\mathbf{i}_x\cos\alpha+\mathbf{i}_y\sin\alpha. \tag{14}$$

At the two ends $z=0$ and $z=z_{\mathrm{f}}$, the boundary conditions for a perfect conductor are $e_x=e_y=0$. However, other end boundary conditions are also of great interest, such as a wave radiating to infinity with no reflection. Therefore the respective end boundary conditions should be assigned when necessary.

The configuration of the longitudinal co-ordinate z is different to that of the transverse ones x and y. Let partial differential with respect to it be denoted by $\partial(\#)/\partial z=(\dot{\#})$ and let the transverse

vectors $\mathbf{q}$ and $\mathbf{p}$ be written as

$$\mathbf{q} = \{ e_x \quad e_y \}^{\mathrm{T}}, \qquad \mathbf{p} = \{ h_y \quad -h_x \}^{\mathrm{T}}. \tag{15}$$

These form a pair of dual vectors. Therefore the variational conditions for e_z and h_z can be carried out first to derive the equations

$$h_z = (\partial e_y/\partial x - \partial e_x/\partial y)/(\mu_0\omega) = (\partial q_2/\partial x - \partial q_1/\partial y)/(\mu_0\omega), \tag{16a}$$

$$e_z = -(\partial h_y/\partial x - \partial h_x/\partial y)/(\varepsilon\omega) = -(\partial p_1/\partial x + \partial p_2/\partial y)/(\varepsilon\omega). \tag{16b}$$

Substituting Eqs. (16a) and (16b) into the variational principle so that the integrand involves only the components of the dual vectors $\mathbf{q}$ and $\mathbf{p}$ gives the Hamiltonian form

$$\Pi(\mathbf{q},\mathbf{p}) = \int \mathrm{Re}\left\{ \int\int_{\Omega} \begin{bmatrix} \mathbf{p}^{\mathrm{H}}\dot{\mathbf{q}} + |\partial p_1/\partial x + \partial p_2/\partial y|^2/(2\varepsilon\omega) - \varepsilon\omega\mathbf{q}^{\mathrm{H}}\mathbf{q}/2 \\ -\mu_0\omega\mathbf{p}^{\mathrm{H}}\mathbf{p}/2 + |\partial q_1/\partial y - \partial q_2/\partial x|^2/(2\mu_0\omega) \end{bmatrix} \mathrm{d}x\,\mathrm{d}y \right\} \mathrm{d}z, \quad \delta\Pi = 0, \tag{17}$$

where $\mathbf{q}$ and $\mathbf{p}$ are the only functions varied in the functional. The merit of using the Hamiltonian system and symplectic geometry is that doing so enables the mathematical method of separation of variables, symplectic eigensolutions, expansion solution, etc., to be used to solve a wide range of problems [11,12], to which periodical waveguide problems are added in this paper. The corresponding Hamiltonian function is

$$\begin{aligned} \mathrm{H}(\mathbf{q},\mathbf{p}) = {} & \varepsilon\omega\mathbf{q}^{\mathrm{H}}\mathbf{q}/2 - (\partial q_1/\partial y - \partial q_2/\partial x)^{\mathrm{H}}(\partial q_1/\partial y - \partial q_2/\partial x)/(2\mu_0\omega) \\ & + \mu_0\omega\mathbf{p}^{\mathrm{H}}\mathbf{p}/2 - (\partial p_1/\partial x + \partial p_2/\partial y)^{\mathrm{H}}(\partial p_1/\partial x + \partial p_2/\partial y)/(2\varepsilon\omega). \end{aligned} \tag{18}$$

The same form of variational principles applies to both structural mechanics and electro-magnetic waveguide problems, so that an *analogy relationship* exists between them.

For the analysis of waveguides formed from homogeneous isotropic material, transmission waves are usually classified as being composed of either transverse electric (TE) or transverse magnetic (TM) waves. Suppose that the material inside the waveguide has $\varepsilon_{(1)} = \varepsilon_0 n_1^2$ where n_1 is its refractive index and $\varepsilon_0 = 8.854 \times 10^{-12}$ F/m is its permittivity in a vacuum. Suppose also that the cladding has permittivity $\varepsilon_{(2)} = \varepsilon_0 n_2^2$, where n_2 is its refractive index, so that certainly $n_2 < n_1$. For periodical waveguides, the in-core material $\varepsilon_{(1)}$ varies periodically with z while $\varepsilon_{(2)}$ can be considered to be invariable. The analysis of such waveguides, e.g., gratings, has important applications.

Plane waveguides are often used in engineering, see Fig. 1. Here the longitudinal co-ordinate is z, x is along the thickness direction, the field is independent of y and there are three layers, namely the substratum, thin film, and cladding [13]. These three layers have refractive indices of, respectively, n_2, n_1 and n_3, such that $n_1 > n_2 \geqslant n_3$. The thin film may be multi-layered, but in this paper only a single-layer periodical waveguide is considered.

2. Analytical solution for a homogeneous plane waveguide with a single thin layer

Each segment is uniform in the z direction and has the three layers described above, see Fig. 1. In the simplest case the substratum and cladding layers can be treated as perfect conductors and the analytical solution can easily be found, whereas for other cases the semi-analytical FE method

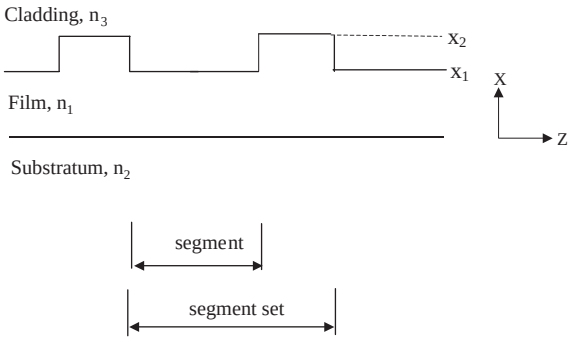

Fig. 1. Plane waveguide.

can be applied. The field solution is composed of TE and TM waves. As a first step, the analytical solution for a homogeneous waveguide is found, as follows.

Because the field is invariant in the y direction,

$$\mathbf{E}(x,z,t) = \mathbf{e}\exp[\mathrm{i}(\kappa z - \omega t)], \qquad \mathbf{H}(x,z,t) = \mathbf{h}\exp[\mathrm{i}(\kappa z - \omega t)]. \tag{19}$$

For isotropic material, the equations can be derived in terms of only one kind of variable, i.e., the components of $\mathbf{E}$ but not of $\mathbf{H}$. Hence Eqs. (3) and (4) become

$$e_y = -(\omega\mu_0/\kappa)h_x, \quad \partial e_z/\partial x - \mathrm{i}\kappa e_x = -\mathrm{i}\omega\mu_0 h_y, \quad \partial e_y/\partial x = \mathrm{i}\omega\mu_0 h_z, \tag{20}$$

$$h_y = (\omega\varepsilon/\kappa)e_x, \quad \partial h_z/\partial x - \mathrm{i}\kappa h_x = \mathrm{i}\omega\varepsilon e_y, \quad \partial h_y/\partial x = -\mathrm{i}\omega\varepsilon e_z \tag{21}$$

and the lateral boundary conditions are

$$e_z = 0, \qquad e_y = 0, \quad \text{when } x = 0 \text{ or } x = x_1, \tag{22}$$

where x_1 is shown in Fig. 1.

The differential equations governing the film of the mth segment (z_{m-1}, z_m) are

$$\mathrm{d}^2 e_y/\mathrm{d}x^2 + (\omega^2\mu_0\varepsilon_m - \kappa_m^2)e_y = 0, \quad \mathrm{d}^2 e_z/\mathrm{d}x^2 + (\omega^2\mu_0\varepsilon_m - \kappa_m^2)e_z = 0 \tag{23a, b}$$

and for pass-bands the analytical problem for this segment is to find the eigenvalue κ_m^2 for a given ω, which can be found from

$$(\omega^2\mu_0\varepsilon_m - \kappa_m^2) = (i\pi/x_1)^2, \quad \text{i.e.,} \quad \omega^2\mu_0\varepsilon_m - (i\pi/x_1)^2 = \kappa_m^2. \tag{24}$$

The corresponding two eigenfunctions are given in Ref. [14] but can also readily be re-derived as

$$\text{TE pass} - \text{band}: \quad \begin{aligned} &e_x = 0, \quad e_y = A_{i,m}\sin(i\pi x/x_1), \quad e_z = 0 \\ &h_x = -(\kappa_m A_{i,m}/\omega\mu_0)\sin(i\pi x/x_1), \quad h_y = 0 \quad (i = 1,2,\ldots), \\ &h_z = -\mathrm{i}(i\pi/x_1\omega\mu_0)A_{i,m}\cos(i\pi x/x_1) \end{aligned} \tag{25a}$$

$$\text{TM pass} - \text{band}: \quad \begin{aligned} &e_x = -\mathrm{i}[\kappa_m x_1/(i\pi)]B_{i,m}\cos(i\pi x/x_1), \quad e_y = 0 \\ &e_z = B_{i,m}\sin(i\pi x/x_1), \quad h_x = 0, \quad h_z = 0 \qquad (i = 1,2,\ldots). \\ &h_y = -\mathrm{i}[\omega\varepsilon_m x_1/(i\pi)]B_{i,m}\cos(i\pi x/x_1) \end{aligned} \tag{25b}$$

Substituting into Eq. (19) easily shows that Eqs. (1)–(4) are satisfied. Here $A_{i,m}$ and $B_{i,m}$ are constants to be determined; the two solutions can be linearly superposed and; the subscript i denotes the wave number of sine and cosine functions.

In addition, it is necessary to consider the stop-band solution, i.e., the case $\omega^2\mu_0\varepsilon_m - (i\pi/x_1)^2 < 0$. Then Eq. (19) should be replaced by

$$\mathbf{E}(x,z,t) = \mathbf{e}\exp[\gamma_m z - \mathrm{i}\omega t], \quad \mathbf{H}(x,z,t) = \mathbf{h}\exp[\gamma_m z - \mathrm{i}\omega t]. \tag{19'}$$

Because γ_m is not a pure imaginary eigenvalue, the solution is in the stop-band and is found to be

$$\text{Stop-band TE}: \quad \begin{aligned} &e_x = 0,\ e_y = A'_{i,m\pm}\sin(i\pi x/x_1),\ e_z = 0,\\ &h_x = \mathrm{i}(\gamma_m A'_{i,m\pm}/\omega\mu_0)\sin(i\pi x/x_1),\ h_y = 0,\\ &h_z = -\mathrm{i}(i\pi/x_1\omega\mu_0)A'_{i,m\pm}\cos(i\pi x/x_1), \end{aligned} \tag{26a}$$

$$\text{Stop-band TM}: \quad \begin{aligned} &e_x = -[\gamma_m 2x_1/(i\pi)]B'_{i,m\pm}\sin(i\pi x/2x_1),\ e_y = 0,\\ &e_z = B'_{i,m\pm}\cos(i\pi x/2x_1),\ h_x = 0,\\ &h_y = -\mathrm{i}[\omega\varepsilon_1 2x_1/(i\pi)]B'_{i,m\pm}\sin(i\pi x/2x_1),\ h_z = 0, \end{aligned} \tag{26b}$$

where $\gamma_m = \pm\sqrt{(i\pi/x_1)^2 - \omega^2\varepsilon_m\mu_0}$ and $A'_{i,m}$, $B'_{i,m}$ are constants to be determined. The $\pm$ sign gives two solutions, where the positive sign solution decays as $z \to -\infty$. However, because the segment is of finite length both solutions are needed when linearly superposing the eigensolutions for the various wave numbers i. Only the TE wave solution is considered below, because the TM solution is similar.

3. The electro-magnetic energy method for the fundamental periodical segment set

A periodical waveguide, e.g., a grating, consists of an infinite number of identical segment sets connected together end to end, to form a chain-type topology. Every set consists of several uniform segments with different cross-sections and/or material properties. Each segment is governed by the above eigensolutions and there must be continuity at their interfaces of the tangential components of E_x, E_y, H_x and H_y.

Without loss of generality, for simplicity, suppose that each segment set has only two uniform segments, with lengths l_1 and l_2, respectively. The fundamental period of a typical such segment set of length $(l_1 + l_2)$ is analyzed first and then the analysis is extended to waveguides which repeat periodically to infinity. Let the origin $z = 0$ be chosen at the interface, so that $-l_1 < z < 0$ for segment 1 and $0 < z < l_2$ for segment 2. Hence the typical segment set = (segment 1 + segment 2 + the interface at $z = 0$) and the solutions for segments 1 and 2 are given by Eqs. (25a) and (25b) with $m = 1$ and 2, respectively.

The interface conditions at $z = 0$ are continuity of E_x, E_y, H_x and H_y. Because solutions (25) and (26) are both sinusoidal in the x direction these conditions are easy to satisfy when the waveguide has constant thickness, i.e., $x_2 = x_1$. However, when the cross-section is stepped at the interface, with $x_2 > x_1$, it is necessary to introduce the additional interface boundary condition

that the tangential electric field component is zero for $x_1 < x < x_2$. So let

$$\mathbf{E} = \tilde{\mathbf{e}} \exp(-\mathrm{i}\omega t), \quad \mathbf{H} = \tilde{\mathbf{h}} \exp(-\mathrm{i}\omega t), \tag{27a, b}$$

where the tilde above symbols denotes that they are functions of (x, y, z), not just the (x, y) of Eq. (19).

For problems with a cylindrical domain of cross-section Ω, the dual vectors $\mathbf{q}$ and $\mathbf{p}$ are

$$\mathbf{q} = \{\, \tilde{e}_x \quad \tilde{e}_y \,\}^{\mathrm{T}}, \qquad \mathbf{p} = \{\, \tilde{h}_y \quad -\tilde{h}_x \,\}^{\mathrm{T}}, \tag{28}$$

from which the Hamiltonian-type variational principle (17) follows. The basis functions of the state vectors can be assigned on the cross-section Ω and the semi-analytical method can be applied. From the variational principle (17) the differential equation set for the longitudinal coordinate z and the corresponding variational principle can be derived.

For Eqs. (25a) and (26a) of segment 2 for TE solutions,

$$q_1 = 0, \quad q_2 = q_{2i}(z) \cdot \sin(i\pi x/x_2), \tag{29}$$

$$p_1 = 0, \quad p_2 = p_{2i}(z) \sin(i\pi x/x_2), \tag{30}$$

where i $(= 1, 2, \ldots)$ are parameters and $q_{2i}(z)$ and $p_{2i}(z)$ are the functions to be determined. Taking unit width in the y direction and integration over Ω gives

$$\Pi_i(q_{2i}, p_{2i}) = \int_0^{l_2} [p_{2i}\dot{q}_{2i} - \omega\varepsilon_2 q_{2i}^2/2 - \mu_0\omega p_{2i}^2/2 + (i\pi/x_2)^2 q_{2i}^2/2\mu_0\omega]\,\mathrm{d}z, \quad \delta\Pi_i = 0, \tag{31}$$

where ε_2 is the permittivity of segment 2 and the factor $(x_2/2)$ has been cancelled. (For segment 1, the integration limits become $(-l_1, 0)$ and the subscript 2 becomes 1.) The varying functions in Eq. (31) are q_{2i} and p_{2i}. Performing the variation for p_{2i} with

$$p_{2i} = \dot{q}_{2i}/(\mu_0\omega) \tag{32}$$

and substituting back into Eq. (31) gives the variational principle for the single variable q_{2i} as

$$U_i(q_{2i}) = \int_0^{l_2} [\dot{q}_{2i}^2/(2\mu_0\omega) - \omega\varepsilon_2 q_{2i}^2/2 + (i\pi/x_2)^2 q_{2i}^2/2\mu_0\omega]\,\mathrm{d}z, \quad \delta U_i = 0,$$

where $U_i(q_{2i})$ is named the *electro-magnetic potential* in this paper, and is determined by the two end variable values $q_{2i}(0)$ and $q_{2i}(l_2)$.

More precisely, the integration lower and upper bounds z_a and z_b (i.e., the two ends of the segment) can also be treated as variables and the functional is then

$$U_i(q_{2i}; z_a, z_b) = \int_{z_a}^{z_b} [\dot{q}_{2i}^2/(2\mu_0\omega) - \omega\varepsilon_2 q_{2i}^2/2 + (i\pi/x_2)^2 q_{2i}^2/2\mu_0\omega]\,\mathrm{d}z, \quad \delta U_i = 0. \tag{33}$$

The differential equation in the domain can be derived from Eq. (33) as

$$\mathrm{d}^2 q_{2i}/\mathrm{d}z^2 + [\omega^2\mu_0\varepsilon_2 - (i\pi/x_2)^2] q_{2i} = 0$$

and the two end boundary conditions are $q_{2i}(z_a) = q_{ai}$ and $q_{2i}(z_b) = q_{bi}$. Solving for $q_{2i}(z)$ gives

$$q_{2i}(z) = [q_{ai}\sin(\kappa_i(z_b - z)) + q_{bi}\sin(\kappa_i(z - z_a))]/\sin(\kappa_i(z_b - z_a)),$$
$$p_{2i}(z) = (\kappa_i/\omega\mu_0)[q_{bi}\cos(\kappa_i(z - z_a)) - q_{ai}\cos(\kappa_i(z_b - z))]/\sin(\kappa_i(z_b - z_a))$$
$$[= \dot{q}_{2i}/\omega\mu_0], \qquad \kappa_i = \sqrt{\omega^2\mu_0\varepsilon_2 - (i\pi/x_2)^2}, \tag{34}$$

i.e., $q_{2i}(z)$ and $p_{2i}(z)$ are functions of q_{ai} and q_{bi}. Substituting into functional (33) gives the electro-magnetic potential $U_i(q_{ai}, q_{bi})$ as the following quadratic function of q_{ai} and q_{bi}:

$$U_i(q_{ai}, q_{bi}) = \begin{Bmatrix} q_{ai} \\ q_{bi} \end{Bmatrix}^{\mathrm{T}} \mathbf{K}_i(z_a, z_b) \begin{Bmatrix} q_{ai} \\ q_{bi} \end{Bmatrix}/2. \tag{35}$$

Here $\mathbf{K}_i(z_a, z_b)$ is a (2×2) symmetric matrix, which appears not to have previously been named and for which the name *electro-magnetic segment stiffness matrix*, or simply *stiffness matrix*, is used in this paper. (In the analogous analytical dynamics problem $U_i(q_{ai}, q_{bi})$ is the action function and in the alternative analogous theory of structural mechanics it is the (dynamic) potential energy [11].) Both $U_i(q_{ai}, q_{bi})$ and $\mathbf{K}_i(z_a, z_b)$ depend on the frequency ω, which is a parameter here, and are usually not expressed explicitly.

For a one-dimensional problem with both ε_2 and μ_0 constant, the (2×2) matrix $\mathbf{K}_i(z_a, z_b)$ can be found analytically, as follows. Carrying out the variation for the electro-magnetic potential of Eq. (33) gives

$$\delta U_i(q_{ai}, q_{bi}) = [(\dot{q}_i/\mu_0\omega)\delta q_i]_{z_a}^{z_b} = [\dot{q}_{bi}\delta q_{bi} - \dot{q}_{ai}\delta q_{ai}]/\mu_0\omega = p_{bi}\delta q_{bi} - p_{ai}\delta q_{ai}. \tag{36}$$

Let $z_a = 0$ and $z_b = l_2$. Then the sub-matrices $\mathbf{K}_i(0, l_2)$ are the (1×1) scalars

$$\mathbf{K}_{iaa} = \mathbf{K}_{ibb} = [\kappa_i \cot(\kappa_i l_2)/(\mu_0\omega)], \quad \mathbf{K}_{iab} = [-\kappa_i/[\mu_0\omega \sin(\kappa_i l_2)]]. \tag{37a}$$

Here the subscript i $(= 1, 2, \ldots, n)$ means that n one-dimensional problems are combined together to give the $(2n \times 2n)$ matrix $\mathbf{K}(0, l_2)$, which can be partitioned as

$$\mathbf{K} = \begin{bmatrix} \mathbf{K}_{aa} & \mathbf{K}_{ab} \\ \mathbf{K}_{ba} & \mathbf{K}_{bb} \end{bmatrix}, \quad \mathbf{K}_{aa} = \mathbf{K}_{aa}^{\mathrm{T}}, \ \mathbf{K}_{bb} = \mathbf{K}_{bb}^{\mathrm{T}}, \ \mathbf{K}_{ba} = \mathbf{K}_{ab}^{\mathrm{T}}, \tag{37}$$

so that $\mathbf{K}_{aa}$, $\mathbf{K}_{bb}$ and $\mathbf{K}_{ab}$ are $(n \times n)$ diagonal matrices given explicitly by Eqs. (37a) and (37) and correspond to a waveguide segment of thickness x_2. For the condition $\omega^2\mu_0\varepsilon_2 - (i\pi/x_2)^2 > 0$ this yields Eq. (34), whereas when $\omega^2\mu_0\varepsilon_2 - (i\pi/x_2)^2 < 0$ the solution is

$$\left.\begin{aligned} q_{2i}(z) &= [q_{ai}\sinh(\gamma_i(z_b - z)) + q_{bi}\sinh(\gamma_i(z - z_a))]/\sinh(\gamma_i(z_b - z_a)), \\ p_{2i}(z) &= (\gamma_i/\mu_0\omega)[q_{bi}\cosh(\gamma_i(z - z_a)) - q_{ai}\cosh(\gamma_i(z_b - z))]/\sinh(\gamma_i(z_b - z_a)) \\ &= \dot{q}_{2i}/\omega\mu_0, \\ \gamma_i &= \sqrt{(i\pi/x_2)^2 - \omega^2\mu_0\varepsilon_2}, \end{aligned}\right\} \tag{34'}$$

and

$$\mathbf{K}_{iaa} = \mathbf{K}_{ibb} = [\gamma_i \coth(\gamma_i l_2)/(\mu_0\omega)], \quad \mathbf{K}_{iab} = [-\gamma_i/(\mu_0\omega \sinh(\gamma_i l_2))]. \tag{37a'}$$

The *Stiffness matrix* is the basic tool used in the FEM analysis of structural mechanics. However, introducing their potential energy and stiffness matrix has enabled electro-magnetic

waveguides to be analyzed by the structural mechanics methodology, especially when combining two consecutive segments. For a uniform waveguide, the cases of $i = 1, \ldots, n$ are solved separately and for each case the stiffness matrix $\mathbf{K}$ is derived analytically, via Eqs. (37) and (37a′), as a diagonal matrix.

However, the structural dynamics analogy shows that the stiffness matrix alone is insufficient for later use because the eigenvalue problem is of vital importance and is well known to need the associated eigenvalue count (EC), which for one segment with clamped end boundary conditions, i.e., $\mathbf{q} = \mathbf{0}$, is defined as

$$EC = J_i(\omega_{\#}^2), \tag{38}$$

where $\omega_{\#}$ is a given frequency and $J_i(\omega_{\#}^2)$ equals the number of eigenvalues ω for which $0 < \omega \leqslant \omega_{\#}$. This implies that the eigensolutions for $J_i(\omega_{\#}^2)$ are internal to the segment.

The Wittrick–Williams (W–W) algorithm [15] was developed to calculate the EC during structural dynamics calculations for complete structures, composed of many members. However, because of the analogy between structural mechanics and wave-guide problems, it can also be applied to eigenvalue problems for electro-magnetic wave-guides composed of many segments as follows. For a constant cross-section segment the analytical solution is derived as above, so that the EC for the jth segment $z_j < z < z_{j+1}$ is

$$J_i(\omega_{\#}^2) = \begin{cases} 0 & \text{when } \omega_{\#}^2\mu_0\varepsilon_j - (i\pi/x_j)^2 \leqslant 0, \\ int\{\kappa_j(z_{j+1} - z_j)/\pi\} & \text{when } \kappa_j^2 = \omega_{\#}^2\mu_0\varepsilon_j - (i\pi/x_j)^2 > 0, \end{cases} \tag{38a}$$

where x_j is its thickness.

However, often $\mathbf{K}_c$ does not have diagonal sub-matrices, e.g., when the semi-analytical method is used. Then $\mathbf{K}_c$ must be found in a single set of operations rather than by the n separate sets used above to find the diagonal elements. Then when two adjacent segments (z_a, z_b) and (z_b, z_c) are combined, see Fig. 2, the sub-matrices of the partitioned stiffness matrix $\mathbf{K}_c$ of the combined segment (z_a, z_c) are computed as [16]

$$\mathbf{K}_{aa}^{(c)} = \mathbf{K}_{aa}^{(2)} - \mathbf{K}_{ab}^{(2)}(\mathbf{K}_{bb}^{(1)} + \mathbf{K}_{aa}^{(2)})^{-1}\mathbf{K}_{ba}^{(2)}, \tag{39a}$$

$$\mathbf{K}_{bb}^{(c)} = \mathbf{K}_{bb}^{(2)} - \mathbf{K}_{ba}^{(2)}(\mathbf{K}_{bb}^{(1)} + \mathbf{K}_{aa}^{(2)})^{-1}\mathbf{K}_{ab}^{(2)}, \tag{39b}$$

$$\mathbf{K}_{ab}^{(c)} = -\mathbf{K}_{ab}^{(1)}(\mathbf{K}_{bb}^{(1)} + \mathbf{K}_{aa}^{(2)})^{-1}\mathbf{K}_{ab}^{(2)}, \quad \mathbf{K}_{ba}^{(c)} = \mathbf{K}_{ab}^{(c)^{\mathrm{T}}}, \tag{39c}$$

and its EC is given by the W–W algorithm as [15,17]

$$J_c(\omega_{\#}^2) = J_1(\omega_{\#}^2) + J_2(\omega_{\#}^2) + s\{\mathbf{K}_{ii}\}, \quad \mathbf{K}_{ii} = (\mathbf{K}_{bb}^{(1)} + \mathbf{K}_{aa}^{(2)}), \tag{39d}$$

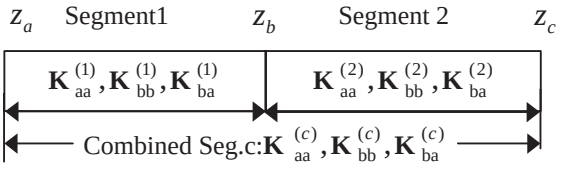

Fig. 2. Segment combination.

where $s\{\mathbf{K}_{ii}\}$ is computed by factorizing the matrix $\mathbf{K}_{ii}$ into $\mathbf{LDL}^{\mathrm{T}}$ and is equal to the number of negative elements in the diagonal matrix $\mathbf{D}$.

The above equations can be applied for arbitrary $(n \times n)$ sub-matrices. However, the variational principle (33) is for a one-dimensional function q_{2i} and so these sub-matrices all become scalars. Then assembling for $i = 1, \ldots, n$ (e.g., see below Eq. (37a)) gives an $(n \times n)$ diagonal matrix.

For $z_a = -l_1$, $z_b = 0$ and $z_c = l_2$, the combination of segments 1 and 2 gives the length of the fundamental period as $(l_1 + l_2)$, with its characteristics described by the electro-magnetic stiffness matrix $\mathbf{K}_c$ related to its two ends. The sub-matrices of $\mathbf{K}_c$ can be computed from Eqs. (39a)–(39d), with the stiffness matrix and EC of segment 2 given by Eqs. (37) and (38), while those of segment 1 are obtained by using l_1 instead of l_2 in these equations. Note that Eqs. (39a)–(39d) are derived for constant cross-section segments. However, in the present application there is a step change of cross-section with $x_1 < x_2$ and the conditions at the junction are

$$e_y(+0) = \begin{cases} e_y(-0), & x < x_1 \\ 0, & x_1 \leqslant x < x_2 \end{cases}, \quad h_x(+0) = \begin{cases} h_x(-0), & x < x_1 \\ 0, & x_1 \leqslant x < x_2 \end{cases} \quad \text{at } z = 0.$$

The variational method can be used to process these junction conditions. According to Eq. (34), the field components of the TE solution at the two ends of segment 2 are

$$\begin{aligned} e_{ya}(+0) &= \sum_{i=1}^{n} q_{ai}^{(2)} \sin(i\pi x/x_2), \quad h_{xa}(+0) = -\sum_{i=1}^{n} (\kappa_i q_{ai}^{(2)}/\omega\mu_0)\sin(i\pi x/x_2), \\ e_{yb}(l_2 - 0) &= \sum_{i=1}^{n} q_{bi}^{(2)} \sin(i\pi x/x_2), \quad h_{xb}(l_2 - 0) = -\sum_{i=1}^{n} (\kappa_i q_{bi}^{(2)}/\omega\mu_0)\sin(i\pi x/x_2), \end{aligned} \tag{40}$$

where $\kappa_i = \sqrt{\omega^2\mu_0\varepsilon_2 - (i\pi/x_2)^2}$, subscript a in $q_{ai}^{(2)}$ represents the left-hand end and superscript (2) indicates that the sine series expansion used is that for thickness x_2. Note that the corresponding sine series expansion for segment 1 is for the different thickness x_1 and so directly connecting the equations of the two segments at their interface is inappropriate.

To correct for this an extended segment 2e is defined as $(-0, l_2 + 0)$ and with its two ends both having thickness x_1. Applying the variational principle to this extended segment requires the boundary condition of the two ends a and b to be

$$\begin{aligned} e_{ya}(-0) &= \begin{cases} \sum_{j=1}^{m} q_{aj}^{(1)} \sin(j\pi x/x_1), & x < x_1, \\ 0, & x_1 \leqslant x < x_2, \end{cases} \\ e_{yb}(l_2 + 0) &= \begin{cases} \sum_{j=1}^{m} q_{bj}^{(1)} \sin(j\pi x/x_1), & x < x_1, \\ 0, & x_1 \leqslant x < x_2. \end{cases} \end{aligned} \tag{41}$$

The sine series expansion of segment 2 has n terms, whereas that for segment 1 has m terms and so does that for segment 2e. Therefore, Eq. (41) is the *given tangential electrical field vector* $\mathbf{e}_{sg}$ in the variational principle (13′). Eq. (34) derives the field in a domain satisfying the differential equations. Therefore it only remains to satisfy the boundary integration (13″), in which Eq. (40) gives $\mathbf{e}$, Eq. (41) gives $\mathbf{e}_{sg}$ and the $\delta\mathbf{h}$ distribution along x again has the form $\sin(j\pi x/x_2)$ $(j = 1, \ldots, n)$, see Eq. (40). Hence the combined variational equation for the tangential electrical

field is derived as

$$\int_0^{x_2} [e_{ya}(+0) - e_{ya}(-0)]\sin(i\pi x/x_2)\,\mathrm{d}x = 0.$$

Carrying out the integration gives

$$q_{ai}^{(2)} = \sum_{j=1}^{m} T_{ij} \cdot q_{aj}^{(1)}, \quad i = 1, \ldots, n \quad \text{or} \quad \mathbf{q}_a^{(2)} = \mathbf{T}\mathbf{q}_a^{(1)},$$

$$T_{ij} = \sin[(j - ix_1/x_2)\pi]/[\pi(jx_2/x_1 - i)] - \sin[(j + ix_1/x_2)\pi]/[\pi(jx_2/x_1 + i)], \tag{42}$$

where the vectors $\mathbf{q}_a^{(2)}$ and $\mathbf{q}_a^{(1)}$ are of orders n and m, respectively, so that the transformation matrix $\mathbf{T}$ has dimension $(n \times m)$. A similar derivation for the right-hand end gives $\mathbf{q}_b^{(2)} = \mathbf{T}\mathbf{q}_b^{(1)}$. Here subscripts a and b represent the left- and right-hand ends, and superscripts (1) and (2) denote series expansion for thickness x_1 or x_2, respectively. Note that as $(jx_2/x_1 - i)\pi, = r$ say, tends to zero $\sin[(j - ix_1/x_2)\pi]/[\pi(jx_2/x_1 - i)] = \sin[rx_1/x_2)/r \to x_1/x_2$ and therefore the coefficients of the matrix $\mathbf{T}$ cannot be singular.

Eq. (37) gives the *electro-magnetic segment diagonal stiffness matrix* $\mathbf{K}_2^{(2)}$ in analytical form, but corresponding to waveguide thickness x_2 and to the two end vectors $\mathbf{q}_a^{(2)}$ and $\mathbf{q}_b^{(2)}$. However, the transformation matrix $\mathbf{T}$ just derived enables it to be transformed into

$$\mathbf{K}_2^{(1)} = \begin{bmatrix} \mathbf{T}^{\mathrm{T}} & \mathbf{0} \\ \mathbf{0} & \mathbf{T}^{\mathrm{T}} \end{bmatrix} \mathbf{K}_2^{(2)} \begin{bmatrix} \mathbf{T} & \mathbf{0} \\ \mathbf{0} & \mathbf{T} \end{bmatrix}, \tag{43}$$

which corresponds to the two end electric field vectors $\mathbf{q}_a^{(1)}$ and $\mathbf{q}_b^{(1)}$ for thickness x_1. Note that although the submatrices of $\mathbf{K}_2^{(2)}$ are diagonal and $(n \times n)$, $\mathbf{K}_2^{(1)}$ is a fully populated $(2m \times 2m)$ matrix. Note too that for a general cross-section waveguide, the semi-analytical method can be used to discretize the cross-section to obtain an n-dimensional electric vector $\mathbf{q}$, after which using the precise integration method gives a stiffness matrix $\mathbf{K}_2^{(2)}$ which, unlike above, is fully populated. However, the semi-analytical method for waveguides and associated precise integration is beyond the scope of this paper, except for the observation that if a cross-section step occurs the $\mathbf{T}$ matrix transformation is still needed.

The transformed stiffness matrix $\mathbf{K}_2^{(1)}$ represents the behaviour of segment 2 but with respect to the reduced cross-section of segment 1. Its EC is unaffected by the transformation, because the boundary condition at the step is $\mathbf{q} = \mathbf{0}$ and so is the same as that used to define $J_i(\omega_{\#}^2)$. However, the fundamental period segment set is composed of both segments 1 and 2, so that the electro-magnetic stiffness matrix $\mathbf{K}_1^{(1)}$ is also required. Substituting $\mathbf{K}_1^{(1)}$ and $\mathbf{K}_2^{(1)}$ into the interval (segment) combination algorithm of Eqs. (39a)–(39d), see Fig. 2, gives the *combined electro-magnetic stiffness matrix* $\mathbf{K}_c$ and $J_c(\omega_{\#}^2)$ for the fundamental period of the waveguide. This computation of $\mathbf{K}_c$ is fundamental to the analysis of a periodical waveguide, e.g., a grating, and corresponds to the *dynamic sub-structural stiffness matrix* $\mathbf{K}_c$ of structural dynamics [17].

Example. The following numerical example shows how to find $\mathbf{K}_c$ for the fundamental period when $\varepsilon_1 = \varepsilon_2 = \varepsilon_0$, $\mu_0\varepsilon_0 = 1/c^2$, $c = 2.998 \times 10^8$ m/s (= the velocity of light), $\omega/c = 4.0 \times 10^6$ m^{-1}, $x_2 = 1.25 \times 10^{-6}$ m, $x_1 = 0.8x_2$ and $l_1 = l_2 = 1 \times 10^{-7}$ m.

Solution. The numbers of expansion terms used for segments 1 and 2 were $m = 4$ and $n = 6$, respectively. Hence Eq. (42) gives the $(n \times m)$ transformation matrix $\mathbf{T}$ as

$$\mathbf{T}^{\mathrm{T}} = \begin{bmatrix} 0.83155 & 0.31049 & -0.10176 & 0.03240 & 0 & -0.01358 \\ -0.17819 & 0.67273 & 0.55042 & -0.09595 & 0 & 0.03145 \\ 0.10742 & -0.22564 & 0.44849 & 0.72425 & 0 & -0.06397 \\ -0.07796 & 0.14416 & -0.18921 & 0.20789 & 0.8 & 0.17009 \end{bmatrix},$$

so that Eqs. (37a) and (37) give

$$\mathbf{K}_1^{(1)} = \begin{bmatrix} \mathrm{diag}_m(\kappa_i^{(1)}/[\mu_0\omega\tan(\kappa_i^{(1)}l_1)]) & \mathrm{diag}_m(-\kappa_i^{(1)}/[\mu_0\omega\sin(\kappa_i^{(1)}l_1)]) \\ \mathrm{diag}_m(-\kappa_i^{(1)}/[\mu_0\omega\sin(\kappa_i^{(1)}l_1)]) & \mathrm{diag}_m(\kappa_i^{(1)}/[\mu_0\omega\tan(\kappa_i^{(1)}l_1)]) \end{bmatrix}, \tag{44a}$$

$$\mathbf{K}_2^{(2)} = \begin{bmatrix} \mathrm{diag}_n(\kappa_i^{(2)}/[\mu_0\omega\tan(\kappa_i^{(2)}l_2)]) & \mathrm{diag}_n(-\kappa_i^{(2)}/[\mu_0\omega\sin(\kappa_i^{(2)}l_2)]) \\ \mathrm{diag}_n(-\kappa_i^{(2)}/[\mu_0\omega\sin(\kappa_i^{(2)}l_2)]) & \mathrm{diag}_n(\kappa_i^{(2)}/[\mu_0\omega\tan(\kappa_i^{(2)}l_2)]) \end{bmatrix}, \tag{44b}$$

$$\kappa_i^{(1)} = \sqrt{\omega^2\mu_0\varepsilon_1 - (i\pi/x_1)^2}, \quad \kappa_i^{(2)} = \sqrt{\omega^2\mu_0\varepsilon_2 - (i\pi/x_2)^2},$$

where $\mathbf{K}_1^{(1)}$ is a $(2m \times 2m)$ matrix. Eqs. (44a) and (44b) are for the pass-bands, whereas the stop-bands are given by

$$\mathbf{K}_1^{(1)} = \begin{bmatrix} \mathrm{diag}_m(\gamma_i^{(1)}/[\mu_0\omega\tanh(\gamma_i^{(1)}l_1)]) & \mathrm{diag}_m(-\gamma_i^{(1)}/[\mu_0\omega\sinh(\gamma_i^{(1)}l_1)]) \\ \mathrm{diag}_m(-\gamma_i^{(1)}/[\mu_0\omega\sinh(\gamma_i^{(1)}l_1)]) & \mathrm{diag}_m(\gamma_i^{(1)}/[\mu_0\omega\tanh(\gamma_i^{(1)}l_1)]) \end{bmatrix}, \tag{44′a}$$

$$\mathbf{K}_2^{(2)} = \begin{bmatrix} \mathrm{diag}_n(\gamma_i^{(2)}/[\mu_0\omega\tanh(\gamma_i^{(2)}l_2)]) & \mathrm{diag}_n(-\gamma_i^{(2)}/[\mu_0\omega\sinh(\gamma_i^{(2)}l_2)]) \\ \mathrm{diag}_n(-\gamma_i^{(2)}/[\mu_0\omega\sinh(\gamma_i^{(2)}l_2)]) & \mathrm{diag}_n(\gamma_i^{(2)}/[\mu_0\omega\tanh(\gamma_i^{(2)}l_2)]) \end{bmatrix}, \tag{44′b}$$

$$\gamma_i^{(1)} = \sqrt{(i\pi/x_1)^2 - \omega^2\mu_0\varepsilon_1}, \quad \gamma_i^{(2)} = \sqrt{(i\pi/x_2)^2 - \omega^2\mu_0\varepsilon_2}.$$

Hence the sub-matrices $\mathbf{K}_{aa}^{(1)}$, $\mathbf{K}_{ab}^{(1)}$ and $\mathbf{K}_{bb}^{(1)}$ of $\mathbf{K}_1^{(1)}$, which appear on the right-hand side of Eq. (39), are computed as

$$\mathbf{K}_{aa}^{(1)} = \mathbf{K}_{bb}^{(1)} = 10^6 \times \mathrm{diag}(9.79481, 10.77063, 12.31731, 14.33589),$$

$$\mathbf{K}_{ab}^{(1)} = 10^6 \times \mathrm{diag}(-10.10291, -9.61915, -8.88198, -7.97522).$$

Similarly the sub-matrices of the $(2n \times 2n)$ matrix $\mathbf{K}_2^{(2)}$ are

$$\mathbf{K}_{aa2}^{(2)} = \mathbf{K}_{bb2}^{(2)} = 10^6 \times \mathrm{diag}(9.67512, 10.30698, 11.32594, 12.68670, 14.33589, 16.21856),$$

$$\mathbf{K}_{ab2}^{(2)} = 10^6 \times \mathrm{diag}(-10.16323, -9.84722, -9.35029, -8.71135, -7.97522, -7.18651).$$

The transformation of Eq. (43) gives the sub-matrices of the $(2m \times 2m)$ matrix $\mathbf{K}_2^{(1)}$ which are required for the right-hand side of Eq. (39) as

$$\mathbf{K}_{aa2}^{(1)} = \mathbf{K}_{bb2}^{(1)} = 10^6 \times \begin{bmatrix} 7.81728 & 0.03861 & -0.06295 & 0.10019 \\ 0.03861 & 8.53600 & 0.13193 & -0.21186 \\ -0.06295 & 0.13193 & 9.63555 & 0.35631 \\ 0.10019 & -0.21186 & 0.35631 & 10.87091 \end{bmatrix} \equiv \mathbf{K}_{aa}^{(2)} = \mathbf{K}_{bb}^{(2)},$$

$$\mathbf{K}_{ab2}^{(1)} = 10^6 \times \begin{bmatrix} -8.08418 & 0.00288 & -0.00190 & -0.00402 \\ 0.00288 & -7.69935 & 0.00091 & 0.01293 \\ -0.00190 & 0.00091 & -7.09821 & -0.03455 \\ -0.00402 & 0.01293 & -0.03455 & -6.28966 \end{bmatrix} \equiv \mathbf{K}_{ab}^{(2)}.$$

Note that the alternative notations given on the left and right of the above equations are necessary because $\mathbf{K}_{aa2}^{(1)}$, $\mathbf{K}_{bb2}^{(1)}$ and $\mathbf{K}_{ab2}^{(1)}$ in the derivation above correspond to the $\mathbf{K}_{aa}^{(2)}$, $\mathbf{K}_{bb}^{(2)}$ and $\mathbf{K}_{ab}^{(2)}$ of Eqs. (39a)–(39c).

Hence the $(m \times m)$ stiffness sub-matrices $\mathbf{K}_{aa}^{(c)}$, $\mathbf{K}_{ab}^{(c)}$ and $\mathbf{K}_{bb}^{(c)}$ of the fundamental period are computed by Eq. (39) as

$$\mathbf{K}_{aa}^{(c)} = 10^6 \times \begin{bmatrix} 3.99921 & 0.01139 & -0.01501 & 0.01845 \\ 0.01139 & 5.97741 & 0.02724 & -0.03378 \\ -0.01501 & 0.02724 & 8.72270 & 0.04586 \\ 0.01845 & -0.03378 & 0.04586 & 11.81172 \end{bmatrix},$$

$$\mathbf{K}_{ab}^{(c)} = 10^6 \times \begin{bmatrix} -4.63754 & 0.01074 & -0.01301 & 0.01217 \\ 0.01054 & -3.83654 & 0.02208 & -0.02009 \\ -0.01276 & 0.02210 & -2.87251 & 0.02214 \\ 0.01351 & -0.02296 & 0.02572 & -1.99045 \end{bmatrix},$$

$$\mathbf{K}_{bb}^{(c)} = 10^6 \times \begin{bmatrix} 4.10640 & 0.04835 & -0.07396 & 0.10894 \\ 0.04835 & 5.46520 & 0.14986 & -0.22472 \\ -0.07396 & 0.14986 & 7.34003 & 0.36538 \\ 0.10894 & -0.22472 & 0.36538 & 9.30125 \end{bmatrix},$$

based on which the energy band analysis of a periodical waveguide can be executed as given below. Note that $m = 4$ and $n = 6$ were used in this example for compactness of presentation, although higher values might be needed depending upon the precision required. An indication of the effects of changing m and n is given in the penultimate paragraph of the next section.

4. Energy band analysis for a grating and eigensolution of a symplectic matrix

After the stiffness matrix $\mathbf{K}_c$ of a single fundamental period has been calculated, the energy band analysis for a periodical waveguide proceeds as follows, by treating the fundamental period as the repeating unit of the periodical waveguide, e.g., of the grating. The electro-magnetic stiffness matrix $\mathbf{K}_c$ and the respective electro-magnetic energy $U_e(\mathbf{q}_a, \mathbf{q}_b)$ are given by

$$\mathbf{K}_c = \begin{bmatrix} \mathbf{K}_{aa} & \mathbf{K}_{ab} \\ \mathbf{K}_{ba} & \mathbf{K}_{bb} \end{bmatrix}, \quad U_e(\mathbf{q}_a, \mathbf{q}_b) = \begin{Bmatrix} \mathbf{q}_a \\ \mathbf{q}_b \end{Bmatrix}^{\mathrm{T}} \mathbf{K}_c \begin{Bmatrix} \mathbf{q}_a \\ \mathbf{q}_b \end{Bmatrix} /2, \tag{45}$$

where superscript (c) has been removed from $\mathbf{K}_{aa}^{(c)}$, etc., and $\mathbf{q}_a$ and $\mathbf{q}_b$ are the two end electrical field vectors of the waveguide fundamental period, being m-dimensional and formed by a Fourier series expansion for the thickness x_1.

In *structural mechanics*, the *periodical waveguide* corresponds to a *sub-structural chain* [18], and a period of the waveguide corresponds to a segment of the sub-structural chain, the dynamic strain energy of which is $U_e(\mathbf{q}_a, \mathbf{q}_b)$. The variational principle for a sub-structural chain of n fundamental segments is

$$\Pi(\mathbf{q}_0, \mathbf{q}_n) = \sum_{i=1}^{i=n} U_{ei}(\mathbf{q}_{i-1}, \mathbf{q}_i), \quad \delta\Pi|_{\mathbf{q}_i,\ i=1,\ldots,n-1} = 0. \tag{46}$$

Using the method in Ref. [16], introducing the dual variable [in electro-magnetic theory (magnetic field$/\omega\mu_0$), see Eqs. (34) and (36)]

$$\mathbf{p}_a = -\partial U_e/\partial \mathbf{q}_a = -(\mathbf{K}_{aa}\mathbf{q}_a + \mathbf{K}_{ab}\mathbf{q}_b), \tag{47a}$$

$$\mathbf{p}_b = -\partial U_e/\partial \mathbf{q}_b = (\mathbf{K}_{ba}\mathbf{q}_a + \mathbf{K}_{bb}\mathbf{q}_b). \tag{47b}$$

From Eq. (46), the equation derived for the ith station is

$$\partial U_i(\mathbf{q}_{i-1}, \mathbf{q}_i)/\partial \mathbf{q}_i + \partial U_{i+1}(\mathbf{q}_i, \mathbf{q}_{i+1})/\partial \mathbf{q}_i = \mathbf{p}_{b,i} - \mathbf{p}_{a,i+1} = \mathbf{0}.$$

This is called the equilibrium equation in structural mechanics, whereas for waveguides it is the tangential magnetic field continuity equation. Eq. (47) expresses the dual vector of the original vectors $\mathbf{q}_a$ and $\mathbf{q}_b$, so that the *state vector* can be composed as

$$\mathbf{v}_j = \{\, \mathbf{q}_j^{\mathrm{T}} \quad \mathbf{p}_j^{\mathrm{T}} \,\}^{\mathrm{T}} \tag{48a}$$

and Eq. (47) can be derived in the form of expressing the right-hand end state vector $\mathbf{v}_b$ in terms of the left-hand end state vector $\mathbf{v}_a$, giving

$$\mathbf{v}_b = \mathbf{S}\mathbf{v}_a, \quad \text{i.e.,} \ \mathbf{v}_{j+1} = \mathbf{S}\mathbf{v}_j, \tag{48b}$$

$$\mathbf{S} = \begin{bmatrix} \mathbf{S}_{11} & \mathbf{S}_{12} \\ \mathbf{S}_{21} & \mathbf{S}_{22} \end{bmatrix}, \quad \begin{matrix} \mathbf{S}_{11} = -\mathbf{K}_{ab}^{-1}\mathbf{K}_{aa}, & \mathbf{S}_{12} = -\mathbf{K}_{ab}^{-1}, \\ \mathbf{S}_{21} = \mathbf{K}_{ba} - \mathbf{K}_{bb}\mathbf{K}_{ab}^{-1}\mathbf{K}_{aa}, & \mathbf{S}_{22} = -\mathbf{K}_{bb}\mathbf{K}_{ab}^{-1}. \end{matrix} \tag{49}$$

The sub-matrices $\mathbf{K}_{aa}$, $\mathbf{K}_{ab}$ and $\mathbf{K}_{bb}$ are $(m \times m)$ and $\mathbf{S}$ is called the *transfer matrix*. It is a *symplectic matrix*, i.e., it satisfies

$$\mathbf{S}^{\mathrm{T}}\mathbf{J}\mathbf{S} = \mathbf{J}, \tag{50}$$

where

$$\mathbf{J} = \begin{bmatrix} \mathbf{0} & \mathbf{I}_m \\ -\mathbf{I}_m & \mathbf{0} \end{bmatrix}, \quad \mathbf{J}^{\mathrm{T}} = \mathbf{J}^{-1} = -\mathbf{J}, \quad \mathbf{J}^2 = -\mathbf{I}_{2m}. \tag{51}$$

Using the method of separation of variables to solve the transfer matrix Eq. (48b) yields the eigenvalue problem

$$\mathbf{S}\boldsymbol{\psi} = \mu\boldsymbol{\psi} \tag{52}$$

This m-dimensional problem is solved [16,18–21] by first finding the eigensolution $(\mu, \boldsymbol{\psi})$ of Eq. (52), so that the solution of the original Eq. (48b) is $\mathbf{v}_j = \mu^j\boldsymbol{\psi}$.

The eigenproblem for a symplectic matrix has the characteristic that if μ is an eigenvalue then so also is μ^{-1}, as follows. Left multiplying Eq. (52) by $\mathbf{S}^{\mathrm{T}}\mathbf{J}$ and using Eq. (50) gives $\mathbf{S}^{\mathrm{T}}(\mathbf{J}\boldsymbol{\psi}) = \mu^{-1}(\mathbf{J}\boldsymbol{\psi})$, which determines that μ^{-1} is an eigenvalue of $\mathbf{S}^{\mathrm{T}}$ and that the corresponding eigenvector is $\mathbf{J}\boldsymbol{\psi}$. However, $\mathbf{S}^{\mathrm{T}}$ and $\mathbf{S}$ have the same eigenvalue spectra, hence the $2m$ eigenvalues of $\mathbf{S}$ can be subdivided into the two classes:

$$(\alpha) \quad \mu_j, \ abs(\mu_j) < 1 \text{ or } abs(\mu_j) = 1 \wedge \ \mathrm{Im}(\mu_j) > 0, \quad j = 1, \ldots, m, \tag{53a}$$

$$(\beta) \quad \mu_{m+j} = \mu_j^{-1}, \quad j = 1, \ldots, m, \tag{53b}$$

where μ_j and μ_{m+j} are called mutually *symplectic adjoint*.

Suppose that $\mathbf{S}$ has two eigensolutions denoted by j and k. Then deriving as follows:

$$\mathbf{S}\boldsymbol{\psi}_j = \mu_j\boldsymbol{\psi}_j, \quad \mathbf{S}\boldsymbol{\psi}_k = \mu_k\boldsymbol{\psi}_k,$$

$$\mathbf{S}^{\mathrm{T}}(\mathbf{J}\boldsymbol{\psi}_j) = \mu_j^{-1}(\mathbf{J}\boldsymbol{\psi}_j), \quad \boldsymbol{\psi}_k^{\mathrm{T}} \cdot \mathbf{S}^{\mathrm{T}} = \mu_k\boldsymbol{\psi}_k^{\mathrm{T}},$$

$$\boldsymbol{\psi}_k^{\mathrm{T}} \cdot (\mathbf{S}^{\mathrm{T}}\mathbf{J}) \cdot \boldsymbol{\psi}_j = \mu_j^{-1}\boldsymbol{\psi}_k^{\mathrm{T}} \cdot \mathbf{J} \cdot \boldsymbol{\psi}_j, \quad \boldsymbol{\psi}_k^{\mathrm{T}} \cdot (\mathbf{S}^{\mathrm{T}}\mathbf{J}) \cdot \boldsymbol{\psi}_j = \mu_k\boldsymbol{\psi}_k^{\mathrm{T}} \cdot \mathbf{J} \cdot \boldsymbol{\psi}_j$$

gives by subtraction of the equations in the final line

$$(\mu_k - \mu_j^{-1})\boldsymbol{\psi}_k^{\mathrm{T}} \cdot \mathbf{J} \cdot \boldsymbol{\psi}_j = 0.$$

Hence, either the two eigensolutions are j and $k = m + j$ and are symplectic adjoint, and hence the constant multipliers can be selected to be *symplectic normalized*, or the eigenvectors must be symplectic orthogonal, i.e.,

$$k \neq m + j \quad \text{and} \quad \boldsymbol{\psi}_k^{\mathrm{T}} \cdot \mathbf{J} \cdot \boldsymbol{\psi}_j = 0, \tag{54}$$

which is called *adjoint symplectic ortho-normality*. Composing a $(2m \times 2m)$ matrix $\boldsymbol{\Psi}$ by using all the eigenvectors gives

$$\boldsymbol{\Psi} = \begin{bmatrix} \boldsymbol{\psi}_1 & \cdots & \boldsymbol{\psi}_m; & \boldsymbol{\psi}_{m+1} & \cdots & \boldsymbol{\psi}_{2m} \end{bmatrix} \tag{55}$$

and then using the adjoint symplectic ortho-normality relationship yields the matrix equation $\boldsymbol{\Psi}^{\mathrm{T}}\mathbf{J}\boldsymbol{\Psi} = \mathbf{J}$, so that $\boldsymbol{\Psi}$ is a symplectic matrix.

When $\mu = \mathrm{e}^{\mathrm{i}\theta}$ is an eigenvalue, then the transfer Eq. (48b) has the solution $\mathbf{v}_j = \mu^j\boldsymbol{\psi}$, and $abs(\mu^j) = abs(\mathrm{e}^{\mathrm{i}(j\theta)}) = 1$. Therefore the vector $\mathbf{v}_j$ does not decay with subscript j and so the solution gives a transmission wave.

When $m = 1$, the eigenequation becomes $\mu^2 - (S_{11} + S_{22})\mu + 1 = 0$. Then for

$$(S_{11} + S_{22})^2 < 4 \quad \text{or} \quad abs[(K_{11} + K_{22})/K_{12}] < 2, \tag{56}$$

a transmission wave appears, i.e., ω is in a pass-band. Treating ω as a variable, changing the inequality sign to an equals sign and solving with respect to ω gives the boundary between pass- and stop-bands.

The general case is multi-dimensional (m-dimensional) and so solving the symplectic eigenvalue problem (52) requires prior solution of a symplectic eigenproblem for a skew-symmetric matrix, as follows. Left multiplying Eq. (52) by $\mathbf{S}^{\mathrm{T}}\mathbf{J}$ gives $\mathbf{S}^{\mathrm{T}}(\mathbf{J}\boldsymbol{\psi}) = \mu^{-1}(\mathbf{J}\boldsymbol{\psi})$ and then using Eq. (50) gives $\mathbf{S}^{-1}\boldsymbol{\psi} = \mu^{-1}\boldsymbol{\psi}$. Hence it follows that

$$\mathbf{A}\boldsymbol{\psi} = (\mu + \mu^{-1})\mathbf{J}\boldsymbol{\psi}, \quad \mathbf{A} = \mathbf{J}(\mathbf{S} + \mathbf{S}^{-1}), \quad \mathbf{A}^{\mathrm{T}} = -\mathbf{A}, \tag{57}$$

where the skew-symmetric nature of matrix $\mathbf{A}$ is readily verified from Eq. (50). Solving to find the pairs of eigensolutions of Eq. (57) gives a 2-D sub-space of the original equation (52), after which the two solutions in the sub-space can conveniently be found. The algorithm for such eigensolution is available, see Refs. [16,18–21]. For the numerical periodical waveguide example given in the previous section, the eigenvalues are found (by again using $m = 4$ and $n = 6$) to be

$$\begin{array}{cccccccc} -0.43114 & -0.77886 & & & & & & \\ & & -0.37586 & -2.66058 & -0.17350 & -5.76373 & & \\ \pm 0.90229\mathrm{i} & \pm 0.62720\mathrm{i} & & & & & & \end{array}$$

where the two complex conjugate pairs of eigenvalues $(-0.43114 \pm 0.90229\mathrm{i})$ and $(-0.77886 \pm 0.62720\mathrm{i})$ are of unit absolute value, which means they lie in a pass-band, whereas the latter two pairs of eigenvalues are the reciprocals of each other, which obeys Eq. (53) for symplectic eigenvalues and so they are in a stop-band. (To save space, the eigenvectors have been omitted above.)

The following additional results are given to show the effects of altering the values of the numbers of expansion terms m and n used and it can be seen that they are very similar to those given above for $m, n = 4, 6$.

$$m, n = 5, 7: \quad \begin{array}{cccccccc} -0.43134 & -0.77971 & & & & & & \\ & & -0.37538 & -2.66397 & -1.7399 & -5.74736. & & \\ \pm 0.90219\mathrm{i} & \pm 0.62615\mathrm{i} & & & & & & \end{array}$$

$$m, n = 9, 9: \quad \begin{array}{cccccccc} -0.43147 & -0.78028 & & & & & & \\ & & -0.37501 & -2.66661 & -0.17408 & -5.74459. & & \\ \pm 0.90213\mathrm{i} & \pm 0.62543\mathrm{i} & & & & & & \end{array}$$

However, if the lengths of segments are changed to $l_1 = l_2 = 0.5 \times 10^{-6}$ m, the eigenvalue spectrum becomes

0.48434

$$-1/53.6491; \quad -53.6491; \quad -1/1922.29; \quad -1922.29; \quad -1/50802.3; \quad -50802.3$$

± 0.87488i;

which has one pair of pass-band eigenvalues and the other pairs are reciprocals of each other.

5. Concluding remarks

Periodical electro-magnetic waveguides have very important applications as gratings and so require careful analysis. It has been shown that symplectic mathematics forms a powerful tool for their analysis, especially when using the analogy between structural mechanics and waveguide problems. It also enables the associated transcendental eigenvalue problem to be solved by using the W–W algorithm. The electro-magnetic stiffness matrix and its associated eigenvalue count have been introduced for the fundamental period of the waveguide and then the variational principle and symplectic eigensolutions have been applied to periodical waveguide problems. Energy band analysis has been carried out on this basis.

Acknowledgements

Thanks are for support from NKBRSF (#G1999032805) of China and also from the UK Engineering and Physical Sciences Research Council (GR/R05437/01). The second author holds a chair at Cardiff University to which he will return upon completion of his appointment at City University of HongKong.

References

[1] C. Kittel, Introduction to Solid State Physics, Wiley, New York, 1986.
[2] A.N. Morozov, V.F. Naumov, Diffraction of electro-magnetic waves by a periodic system of coupled iris waveguides, Soviet Journal of Communications Technology & Electronics 37 (1992) 63–69.
[3] S. Selleri, M. Zoboli, Performance comparison of finite-element approaches for electromagnetic waveguides, Journal of the Optical Society of America A—Optics Image Science and Vision 14 (1997) 1460–1466.
[4] D.G. Pedreira, P. Joly, A method for computing guided waves in integrated optics, SIAM Journal on Numerical Analysis 39 (2001) 596–623.
[5] S.G. Mao, M.Y. Chen, A novel periodic electromagnetic bandgap structure for finite-width conductor-backed coplanar waveguides, IEEE Microwave and Wireless Components Letters 11 (2001) 261–263.
[6] A. Bermudez, D.G. Pedreira, P. Joly, A hybrid approach for the computation of guided modes in integrated optics, Advances in Computational Mathematics 16 (2002) 229–261.
[7] S. Ramo, J.R. Whinnery, Th. Van Duzer, Fields and Waves in Communication Electronics, 3rd Edition, Wiley, New York, 1994.
[8] A. Yariv, Quantum Electronics, 2nd Edition, Wiley, New York, 1975.
[9] J.A. Stratton, Electro-magnetic Theory, McGraw-Hill, New York, 1941.

[10] W.X. Zhong, Symplectic system of electro-magnetic wave-guide, Journal of Dalian University of Techology 41 (2001) 379–387 (in Chinese).
[11] W.X. Zhong, A New Systematic Methodology for Theory of Elasticity, Dalian University of Technology Press, Dalian, 1995 (in Chinese).
[12] W.X. Zhong, J.H. Lin, J.P. Zhu, Computation of gyroscopic systems and symplectic eigensolutions of skew-symmetric matrices, Computers & Structures 52 (1994) 999–1009.
[13] Z.Q. Cao, Method of Transfer Matrix in Optical Wave-guides, Shanghai Jiao-Tong University Press, Shanghai, 2000 (in Chinese).
[14] W.X. Zhong, Symplectic analysis for electro-magnetic wave guide with varied cross sections, Chinese Quarterly of Mechanics 22 (2001) 273–280.
[15] W.H. Wittrick, F.W. Williams, A general algorithm for computing natural frequencies of elastic structures, Quarterly Journal of Mechanics and Applied Mathematics 24 (1971) 263–284.
[16] W.X. Zhong, H.J. Ouyang, Z.C. Deng, Computational Structural Mechanics and Optimal Control, Dalian University Technology Press, Dalian, 1993 (in Chinese).
[17] A.Y.T. Leung, Dynamic Stiffness & Sub-Structures, Springer, London, 1993.
[18] W.X. Zhong, F.W. Williams, On the localization of the vibration mode of a sub-structural chain-type structure, Proceedings of the Institution of Mechanical Engineers, Part C 205 (1991) 281–288.
[19] W.X. Zhong, F.W. Williams, Wave propagation for repetitive structures and symplectic mathematics, Proceedings of the Institution of Mechanical Engineers, Part C 206 (1992) 371–379.
[20] W.X. Zhong, F.W. Williams, The eigensolutions of wave propagation for repetitive structures, Structural Engineering and Mechanics 1 (1993) 47–60.
[21] W.X. Zhong, F.W. Williams, On the direct solution of wave propagation for repetitive structures, Journal of Sound & Vibration 181 (1995) 485–501.